

A Proliferation-Resistant Lead-Cooled Reactor for Transmutation of TRU and LLFP

Y. Kim, S. J. Kim, and T. Y. Song
Korea Atomic Energy Research Institute,
150 Deokjin-dong, Yesong-gu, Daejeon 305-353, Korea

Abstract

The transmutation of TRU and LLFP (Tc-99 and I-129) in a 900 MWth lead-cooled reactor has been studied based on a proliferation-resistant, practical fuel cycle. For a high-performance fast reactor core, we introduce a new fuel assembly design concept, where B_4C burnable absorbers and neutron streaming tubes are adopted. It is shown that with the new fuel assembly design both the burnup reactivity swing and peak fast neutron fluence can be substantially reduced. In addition, the reactor core can be designed with single fuel enrichment. To investigate the thermal-hydraulic behavior of the fuel assembly, a subchannel analysis is performed for the peak power assembly. Also, a sensitivity study is performed for the uranium removal rate to identify its impacts on the TRU transmutation capability and core characteristics. Tc-99 and I-129 are transmuted in moderated assemblies loaded into the reflector zone. For an efficient transmutation of Tc-99 and I-129, a double-annular LLFP target enclosing a $ZrH_{1.78}$ moderator is used. A balanced transmutation of TRU and LLFP can be done in a core and the transmutation rates of Tc-99 and I-129 are found out to be $\sim 6.9\%$ /year and $\sim 6.0\%$ /year, respectively.

I. Introduction

For sustainable development of nuclear energy in the future, it is generally recognized that the current spent nuclear fuel (SNF) issue needs to be properly resolved. One of the practical, promising approaches to the SNF problem is the transmutation of long-lived radioactive nuclides such as transuranics (TRUs) and long-lived fission products (LLFPs) in nuclear reactors, in which the TRUs are consumed as nuclear fuel. It is well perceived that fast neutron reactors are required for an efficient and balanced TRU transmutation. In this paper, a lead-cooled fast reactor is studied for the TRU and LLFP transmutation.

In commercial spent fuels from PWRs, the mass fraction of TRUs is very small, usually 1.0 ~ 1.4 w/o of the total fuel mass, depending on the fuel burnup, and most of the PWR spent fuel is uranium. Therefore, for a fast and efficient transmutation of TRUs, they need to be separated from the spent fuel. In addition, a TRU recycling is usually necessary since a perfect burnup of TRUs is impossible in a nuclear reactor. Thus, spent fuel reprocessing is essential and avoidable in the transmutation reactor. Generally, a very high degree of uranium removal rate (more than 99.9%) from the SNF is presumed and most of fission products are removed for the TRU transmutation.[1,2] This high-order separation requirements give rise to the proliferation concern.

Among several reprocessing methods, the pyroprocessing technology is being studied for the transmutation purpose in Korea since it is generally considered to be proliferation-resistant and might be economically competitive. Unfortunately, the envisaged performance of the currently-favored pyroprocessing technology is far behind the targeted goals in terms of the uranium and rare earth (RE) elements removal rates. In this work, we have investigated the feasibility of TRUs and LLFPs transmutation in a lead-cooled reactor with a practically-constrained, proliferation-resistant closed fuel cycle from the viewpoint of the uranium and RE removal rate.

Based on the performance of the current pyrotechnologies, in this work, it is assumed that only 97% of uranium and 90% of RE could be removed from the spent fuel of PWRs.[3] Also, to simplify the whole fuel cycle and fabrication processes, from the spent fuel of the transmuter itself, only fission products are removed (90% RE removal) and all the remaining elements are recycled into the transmuter. In this process, the actinide recovery rate is assumed to be 99.9%, which might

be considered to be a practical goal. In the transmuter, Tc-99 and I-129 LLFPs are also to be transmuted since they are major dose contributors in a geological repository of SNF and are transmutable. The LLFP Cs-135 is not transmuted in this work because the transmutation efficiency is very poor. Figure 1 shows the schematic fuel cycle utilized in this paper. It is worthwhile to note that Cs and Sr elements are stored in a decay storage before they are finally disposed of in a repository.

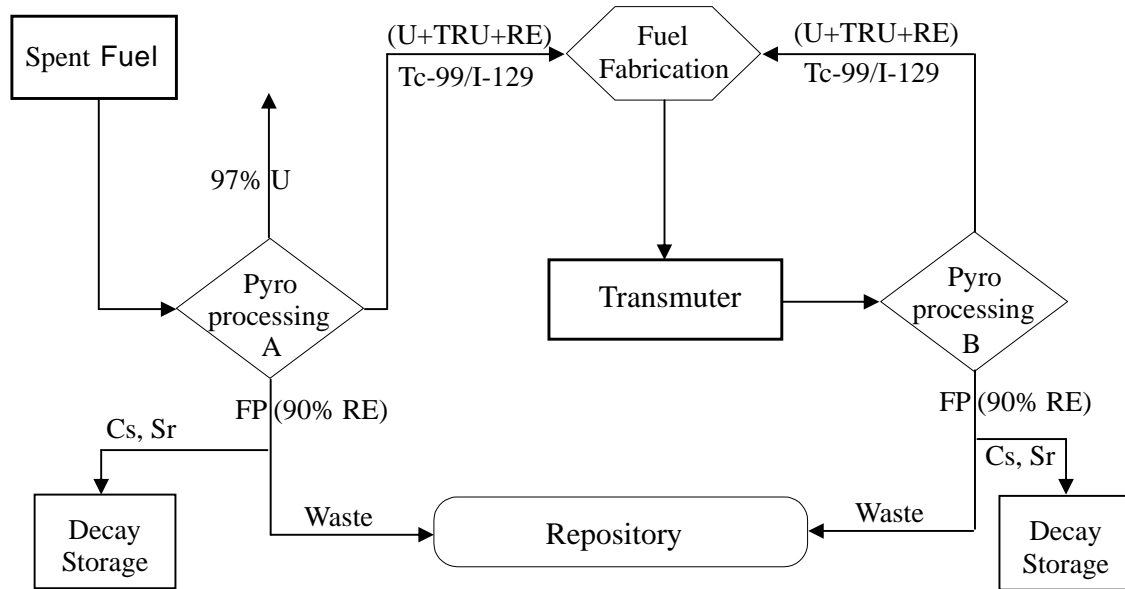


Fig. 1. Schematic fuel cycle for transmutation of TRU and LLFP

In Section II, core design features of the transmuter are described. Section III contains the results for the TRU-only transmutation and both the TRU and LLFP are transmuted in Section IV. Finally, conclusions are given in Section V.

II. Lead-Cooled Reactor Core

Lead-Bismuth-cooled reactors have been studied due to its several advantage over the conventional sodium cooled fast reactors: high boiling temperature, benign chemical activity etc. However, the LBE coolant a few crucial drawbacks such as corrosion problems, very high Po-210 activity, possible reaction between water and bismuth, in spite of its relatively low melting temperature (~ 126 °C). Consequently, pure lead is being investigated as a coolant although the lead coolant is also subject to the corrosion issue, albeit a little less corrosive, and it has a rather high melting point (~ 327 °C). It is expected that coolant freezing would not be an issue in a lead-cooled reactor with a high operating temperature.

In this paper, a 900 MWth lead-cooled reactor has been considered for the transmutation study. As shown in Fig. 2, the reactor core is divided into 3 zones and comprises 192 ductless hexagonal fuel assemblies. In a lead-cooled reactor, the coolant volume fraction should be quite high to remove heat efficiently. This leads to a simple ductless fuel assembly design in this work. In the fuel assembly, there are 204 fuel rods and 13 tie rods (TRs). TRs are basically empty tubes and they are used to hold the grid spacers supporting fuel rods. Two types of control rods are designed, one is in the core and the other one in the reflector. Lead is also used as the reflector material in the core. Although fuel assemblies are ductless, the reflector and shield assemblies have a duct for the coolant flow control.

Fuel is the conventional metallic alloy of U-TRU-Zr with a lead bonding. The height of the active core is 124 cm and the pitch-to-diameter (P/D) ratio of fuel rods is 1.41. Taking into account

the relatively high melting temperature of lead, the coolant inlet temperature was set to 420 °C and the coolant outlet temperature was determined to be 540 °C for a high thermal efficiency, resulting in an average coolant speed of ~1.66 m/sec. Special FP assemblies containing Tc-99 and I-129 targets are loaded into the reflector zone.

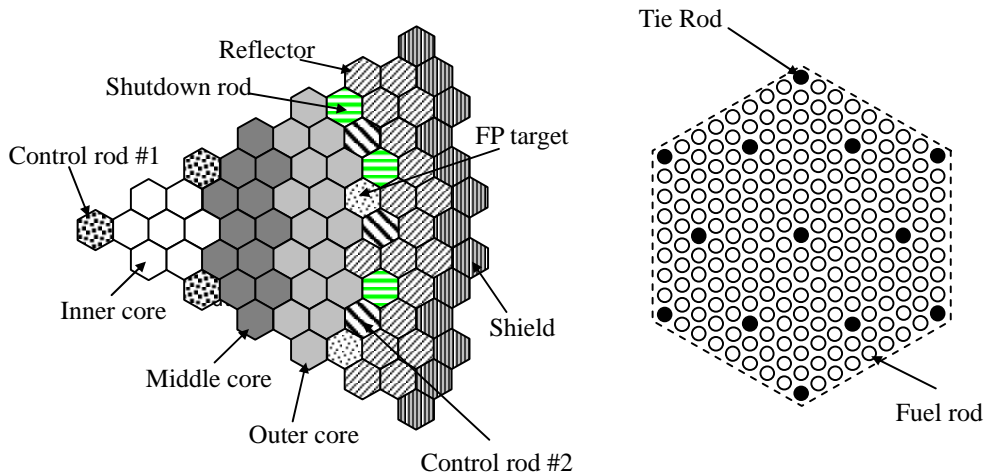


Fig. 2. Configurations of reactor core and ductless fuel assembly

When a core is mainly loaded with a TRU fuel from PWRs, the core has a large burnup reactivity swing. Also, in a fast neutron spectrum core, the core design and performance are tightly constrained by the fast neutron fluence limit. In a TRU burner, the fuel enrichment needs to be adjusted region-wise for the power distribution control and this results in several types of fuel rods in the core. Basically, it is desirable that the number of fuel rod types should be minimized for a lower fuel fabrication cost and an easier quality control of the fuel.

In order to solve the above-mentioned problems, a new fuel assembly design has been introduced in this work. First, B-10 (in the form of B₄C) is used as a burnable absorber (BA) to reduce the burnup reactivity swing. The BA is loaded inside 13 TRs with top and bottom cutbacks as shown in Fig. 2. The objective of the cutbacks is twofold, one is to enhance the B-10 depletion rate and the other one is to minimize the peak fast fluence, thereby extending the lifetime of the fuel assembly. The peak fast neutron fluence limit is a limiting design fast in a lead-cooled fast reactor. The BA loading with the top/bottom cutbacks flattens the axial power distribution and effectively reduces the peak neutron fluence, which usually appears in the core mid-plane. In addition to the BA rods, we have also introduced the so-called neutron streaming tube (NST) as another design measure for power distribution control in the core. The NST is simply an empty tube, which enhances the neutron stream effect and thus may reduce the void reactivity of the core.[4,5] Table I shows the assembly design data.

The B₄C option may significantly reduce the burnup reactivity swing, but makes the coolant void reactivity less favorable. Meanwhile, the NST approach may reduce the void reactivity, but it increases the peak linear power since it replaces fuel rods. Meanwhile, the NST concept has little impact on the relatively large burnup reactivity swing of a TRU transmuter. To make best use of the two concepts, they have been combined in this study. In the inner core, the B₄C BA is loaded and 18 NSTs are placed per fuel assembly, and the middle core has 12 NSTs/assembly and B₄C BA rods. However, no NSTs and no B₄C BAs are applied in the outer core.

In Ref. 5, it is shown that the new design can be effectively applied to a lead-cooled breakeven core with a single fuel enrichment. The single fuel enrichment significantly enhances the proliferation resistance of a breakeven fast reactor since Pu enrichment adjustment is not required. In a TRU burner, the need of a single TRU enrichment is rather weak in terms of the proliferation resistance since TRU is already treated as a separate material. Nevertheless, the single TRU

enrichment provides some benefits from the fuel fabrication and management points of view. We provide a TRU burner core design with a single fuel enrichment in the next section.

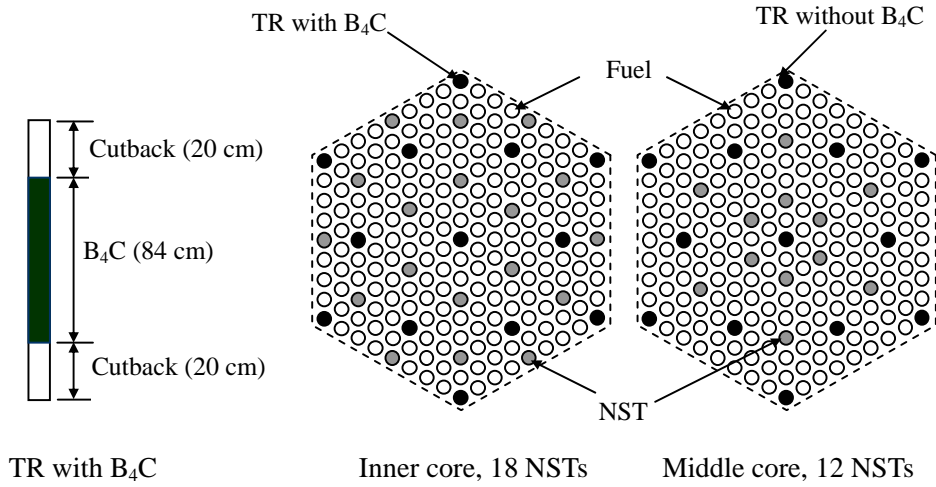


Fig. 2. Fuel assemblies with B_4C burnable absorbers and NSTs

Table I. Ductless fuel assembly design

| | |
|----------------------------|-------------------------|
| Fuel material | U-TRU-Zr metallic alloy |
| Cladding, TR, NST material | HT9 |
| No. of fuel pins | $204 - N_{NST}^*$ |
| No. of TRs | 13 |
| Pin diameter, cm | 0.88 |
| Cladding thickness, cm | 0.057 |
| P/D ratio | 1.41 |
| Fuel smear density, %TD | 75 |
| Diameter of TR, cm | 0.96 |
| Tube thickness of TR, cm | 0.13 |
| Diameter of NST, cm | 0.96 |
| Tube thickness of NST, cm | 0.057 |
| Active length, cm | 124 |
| Inter-assembly gap, cm | 0.32 |
| Assembly pitch, cm | 18.393 |

* No. of NSTs

All the neutronic analyses in this paper have been done with the REBUS-3[6]/DIF3D[7] code system and the ENDF-B/VI cross section data. In the DIF3D analysis, a nodal diffusion method has been used with 9-group cross sections, which are obtained from the TRANSX[8]/ TWODANT[9] code system.

III. TRU-only Transmutation Performance

With the aforementioned core design and fuel cycle concepts, a one-year-cycle core has been designed to have 310 effective full power days (i.e., 85% capacity factor). As in the typical fast reactor, the scattered fuel reloading is utilized in the core. For the inner and middle zones, a 6-batch fuel management is used and a 7-batch one is applied to the outer zone for a high discharge burnup. In this study, the feed fuel material is obtained by removing 97% uranium and 90% RE from a PWR spent fuel with a burnup of 47 GWD/MTU and a 20-year cooling time. It was assumed that fission products except RE could be completely removed from the SNF. The composition of the

feed fuel was calculated with the ORIGEN2[10] code for a UO₂ fuel of an enrichment of 4.4 w/o U-235. It is worthwhile to note that, in one tone of SNF with a 47 GWD/MTU burnup, the mass fractions of uranium, TRU and RE are 93.8%, 1.32%, and 1.40%, respectively.

Two types of core have been analyzed for a comparison purpose. One is based on the design concept in Section II and the other one is the conventional design with a zone-dependent fuel enrichment. In the new design, the single fuel enrichment concept has been employed for a simplified fuel cycle. In this case, for the power distribution, 75%-enriched and 45%-enriched B₄C absorbers were loaded inside TRs in the inner and middle cores, respectively. Table II shows the major core parameters of equilibrium cycles of the two cores.

Table II clearly shows that the peak fast neutron fluence in the conventional design exceeds the limiting value (4.0×10^{23} for the HT9 steel), while the peak fluence in the new approach is significantly smaller than the design limit. This is mainly due to the BA rod with the top/bottom cutbacks. It is important to note that the burnup reactivity swing in the new design is reduced by about 59% compared with the conventional core design. The substantially reduced reactivity swing is largely attributed to the depletion of the B-10 isotope. Although B-10 is a relatively good burnable absorber, its depletion rate is fairly slow in a fast reactor, thus the fuel discharge burnup is reduced by about 23%. The discharge burnup of B-10 is about 68% in the core. On the other hand, introduction of the B₄C BA makes the core void reactivity less favorable: the void reactivity in the active core is increased by about 87% relative to the conventional design. This is mainly because the absorption cross section of B-10 decreases as the neutron spectrum becomes harder.

Table II shows that the neutron generation time is noticeably shorter in the new design due to the B₄C BA in the new core and the β_{eff} values in the two cores are just slightly smaller than that of the conventional fast cores. It is expected that the control of the core would not be very challenging as in the pure TRU burner core with a much smaller delayed neutron fraction.

Table II. Summary of core characteristics

| Parameter | Value | |
|---|----------------------|----------------------|
| | New | Conv. |
| Fuel composition (U/TRU/RE/Zr), w/o | 63.5/19.6/0.5/16.4 | *) |
| Reactivity swing, pcm | 913 | 2,212 |
| Delayed neutron fraction (β_{eff}) | 0.00314 | 0.00314 |
| Neutron generation time, μsec | 0.50 | 0.80 |
| Core power density, W/cc | 129 | 129 |
| Avg. linear power, W/cm | 193 | 185 |
| Fuel discharge burnup, a/o | 9.0 | 11.8 |
| Peak fast fluence (>0.1 MeV), n/cm^2 | 3.7×10^{23} | 4.6×10^{23} |
| Heavy metal consumption (U/TRU), kg/cycle | 196/92 | 196/92 |
| Heavy metal inventory (BOC/EOC), kg | 18,466 / 18,176 | 14,006 / 13,718 |
| BOC B-10 inventory, kg | 29.8 | --- |
| Void reactivity (100% active core), pcm | 4,308 | 2,306 |

*) Inner core : 49.5/15.7/0.2/34.6
 Middle core: 52.6/17.3/0.4/29.6
 Outer core : 56.1/19.5/0.8/23.7

As shown in Table II, the fuel composition in the new design is not much different from the conventional fast reactor fuel with a 10w/o Zr. Thus we think that the required fuel technology could be developed by extending the current metal fuel technologies. However, in the conventional core design, it is considered that a new metal fuel technology needs to be developed due to the significant difference in the composition. It is noteworthy that the RE fraction in the fuel is not negligible since its removal rate in the fuel reprocessing is only 90%. In Table III, fuel composition vectors are shown for the new design in an equilibrium cycle.

Although 97% of uranium in the SNF was removed, the majority of the feed material is still uranium, about 68 w/o. Consequently, the TRU transmutation capability of the core is about 1/3 of a transmuter loaded with pure TRUs.

In Fig. 3, the assembly power distribution is shown for an equilibrium cycle of the new core design. In the newly introduced design method, the number of fuel rods in an assembly is different in the three zones. In order to investigate the thermal hydraulic behavior in each assembly type, we have performed a subchannel analysis with the MATRA[11] code for the assemblies with the peak power in each zone. The results are summarized in Table IV.

In a lead-cooled reactor, it is generally required that the coolant speed should not exceed 2.0 m/sec due to the corrosion and erosion effects. Table IV shows that the maximum coolant speed satisfies the requirement. Actually, the peak coolant speed takes place in the peripheral region of an assembly and it is expected that the maximum speed may be reduced by optimizing the assembly design. In order to limit the corrosion of the cladding, the cladding surface temperature needs to be kept as low as possible. In the core, the maximum cladding outer surface temperature occurs at the middle core. The cladding temperature could be further reduced by optimizing the power distribution. It can be easily done by increasing the B-10 loading in the middle core and/or by differentiating the B-10 enrichment in a zone. In this work, the MATRA analysis was performed on the assumption that the coolant mass flow rate is identical in all the assemblies. However, the coolant flow rate might be adjusted zone-wise. This may lead to a reduced coolant/cladding temperature in the inner and middle zones.

Table III. Fuel compositions (w/o) in an equilibrium cycle (new design)

| Isotope | Feed | Charge | Discharge |
|---------|---------|--------|-----------|
| U-234 | 0.017 | 0.17 | 0.15 |
| U-235 | 0.60 | 0.15 | 0.087 |
| U-236 | 0.40 | 0.43 | 0.39 |
| U-238 | 64.80 | 75.24 | 68.86 |
| Np-237 | 2.09 | 0.62 | 0.41 |
| Pu-238 | 0.70 | 0.87 | 0.79 |
| Pu-239 | 15.70 | 10.48 | 8.92 |
| Pu-240 | 6.95 | 7.36 | 6.65 |
| Pu-241 | 1.34 | 0.83 | 0.76 |
| Pu-242 | 1.42 | 1.44 | 1.30 |
| Am-241 | 2.25 | 0.10 | 0.71 |
| Am-242m | 0.0053 | 0.056 | 0.056 |
| Am-243 | 0.37 | 0.43 | 0.39 |
| Cm-242 | 1.28E-5 | 0.0020 | 0.027 |
| Cm-243 | 0.0010 | 0.0020 | 0.0021 |
| Cm-244 | 0.075 | 0.26 | 0.27 |
| Cm-245 | 0.0078 | 0.079 | 0.079 |
| Cm-246 | 0.0011 | 0.045 | 0.045 |
| RE | 3.28 | 0.55 | 2.26 |
| FP* | 0.0 | 0.0 | 7.84 |

* without RE

Up to now, it was assumed that 97% uranium and 90% RE are removed from SNF for a practical fuel cycle, which might be achievable with the current pyrotechnologies. We have also done a sensitivity study for the uranium removal rate to identify its impacts on the core characteristics and transmutation performance. In this case, the RE removal rate is fixed at 95% (a targeted RE separation index) and the core design was done with the conventional fuel enrichment adjustment scheme. The results are summarized in Table V.

In Table V, it is observed that the fuel inventory monotonically decreases and fuel discharge burnup increases with the uranium removal rate. One can also see that the burnup reactivity swing increases and the effective delayed neutron fraction decreases as the uranium removal rate increases.

Table V clearly shows that the core design would be very difficult with pure TRU fuels due to the small delayed neutron fraction and a large burnup reactivity swing although TRU transmutation rate is fairly high. Meanwhile, it was found that the core can hardly be a TRU transmuted if the uranium removal rate is smaller than 90% because of high conversion ratio. The neutron generation time increases as the uranium content is high in the fuel.

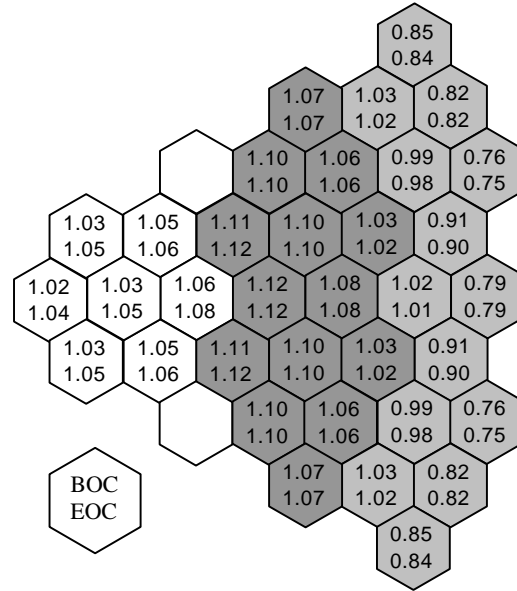


Fig. 3. Relative assembly power distribution in an equilibrium cycle (new design)

Table IV. TH analysis for peak power assemblies

| Parameter | Inner core | Middle Core | Outer core |
|---|-------------|-------------|-------------|
| Peak power, MW | 5.25 | 5.46 | 5.20 |
| Coolant speed (avg./max), m/sec | 1.69 / 1.82 | 1.68 / 1.81 | 1.66 / 1.78 |
| Coolant exit temperature (avg./max.), °C | 554 / 579 | 561 / 580 | 553 / 564 |
| Peak cladding outer surface temperature, °C | 599 | 601 | 582 |
| Peak fuel temperature, °C | 703 | 703 | 675 |
| Pressure loss, Mpa | 0.196 | 0.195 | 0.193 |

Table V. Impacts of uranium removal rate on core characteristics

| U removal, % | 99.99 | 99.9 | 99.0 | 97.0 | 94.0 | 90.0 |
|-------------------------------|-------|------|------|------|------|------|
| Heavy metal loading, ton | 4.16 | 4.83 | 9.42 | 13.9 | 16.4 | 17.8 |
| Fuel burnup, a/o | 36.9 | 32.5 | 18.0 | 12.6 | 10.8 | 9.9 |
| Reactivity swing, %Δk | 7.64 | 7.18 | 4.11 | 2.21 | 1.49 | 1.12 |
| β_{eff} , pcm | 264 | 268 | 293 | 314 | 324 | 330 |
| Neutron generation time, μsec | 1.08 | 1.05 | 0.91 | 0.80 | 0.74 | 0.72 |

IV. Simultaneous Transmutation of TRUs and LLFPs

In this section, both TRU and LLFP are to be transmuted in the core. Among LLFPs, Tc-99 and I-129 are transmuted due to their high toxicity and good mobility in a geological repository. In this

work, a metallic Tc-99 target is used and I-129 is loaded in the CaI_2 form. The iodine target is directly formed with the elemental iodine extracted from the SNF, which includes both I-127 (23%) and I-129 (77%) isotopes.

Regarding the LLFP transmutation, many previous studies have shown that a moderated target assembly is preferable in terms of the transmutation rate. Especially, Ref. 12 showed that an annular target enclosing a moderator is much better than the typical solid type target since the self-shielding effect could be minimized and the annular target itself can be used as a thermal neutron filter, which mitigates the local power peaking problem in neighboring fuel assemblies. Also, the same work indicated that LLFP transmutation in reflector zone is favorable in terms of the neutron economy and the core safety. Furthermore, a related work in Ref. 5 showed that a double-annular LLFP target is a promising Tc-99/I-129 target configuration, where annular Tc-99 and I-129 targets are simultaneously loaded in a single rod. Based on the results of Refs. 5 and 12, the double-annular target is also used for the transmutation of Tc-99 and I-129 in this paper. A schematic of the LLFP assembly is depicted in Fig. 4. In the LLFP assembly, $\text{ZrH}_{1.78}$ is used as a moderator. It is worthwhile to note that the central moderator is replaced with the HT9 steel along the boundary adjoining fuel assemblies to reduce the possible power peaking problem due to thermal neutrons.

As shown in Fig. 4, LLFP pins are arranged in a tight triangular lattice inside a duct. Design data for the LLFP assembly are given in Table VI. Note that a tight lattice is employed for the LLFP pins since the cooling requirement is fairly low for the LLFP pins.

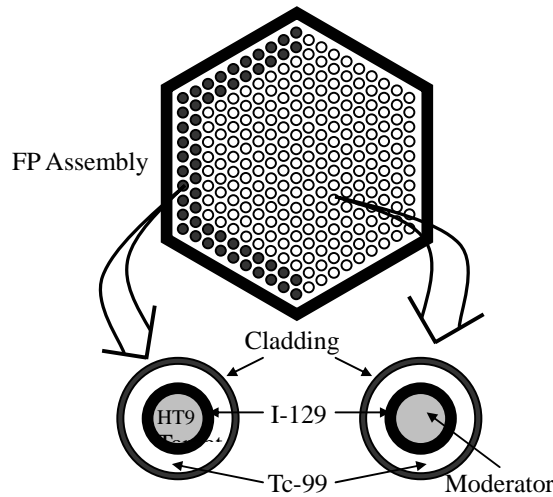


Fig. 4. Configuration of LLFP assembly

Table VI. LLFP assembly design data

| | |
|---|---------------|
| No. of pins per assembly | 217 |
| Pin diameter, cm | 1.05312 |
| Cladding thickness, cm | 0.055 |
| P/D ratio | 1.08 |
| Duct outside flat-to-flat, cm | 18.093 |
| Duct wall thickness, cm | 0.54 |
| Inter-assembly gap, cm | 0.3 |
| Assembly pitch, cm | 18.393 |
| Radius of moderator, cm | 0.39832 |
| Radii of CaI_2 target (inner, outer), cm | 0.4033/0.4356 |
| Radii of Tc-99 target (inner, outer), cm | 0.4406/0.4666 |

The code systems used in this work is basically for a fast spectrum core. Thus, we analyzed the moderated LLFP assembly with a Monte Carlo code called MCCARD[13] in a spectral geometry

including fuel and reflector assemblies to evaluate the multi-group homogenized cross sections for the LLFP assembly. In the Monte Carlo analysis, the power peaking phenomenon was also assessed and the local power peaking factor was calculated to be about 1.3 in a fuel assembly neighboring the LLFP assembly. A power peaking factor 1.3 in a peripheral fuel assembly is considered to be acceptable since the power density is generally low.

When both TRU and LLFP are simultaneously transmuted in a core, it is desirable that the supporting ratios (SRs) for TRU and LLFP should be equal such that neither TRU and LLFP are accumulated. For the 900 MWth core in the work, SR for TRU is about 1.2 and the core needs to transmute 13.7 kg of Tc-99 and 3.2 kg of I-129 every cycle.

In Table VII, the results of the TRU and LLFP transmutation are summarized for an equilibrium cycle. In the analysis, 12 LLFP assemblies are loaded in the reflector zone as shown in Fig.1 and they are irradiated during 7 consecutive cycles. For an effective transmutation of LLFPs, the LLFP targets are only loaded in the central region with the 20-cm top/bottom cutback zones just like the BA rods. In the previous TRU-loaded core, the core design was performed such that all the fuel rods have the same fuel enrichment. However, it was found that too much amount of B-10 needs to be loaded in the inner and middle zone for a single fuel enrichment when the LLFP assemblies are loaded in reflector, aggravating the core performance such as fuel discharge burnup and void reactivity. Also, the Zr content should be smaller than 10% if B-10 loading is too high. Thus, the enrichment split concept is also introduced for the power distribution control in this case, while keeping the same fuel assembly design as in the TRU-only-loaded core. In other words, the number of NSTs and B₄C enrichments in the inner and middle cores are the same as in the previous core design in Section III.

Table VII. Summary of TRU & LLFP transmutation

| Parameter | Value |
|---|--|
| Fuel composition (U/TRU/RE/Zr), w/o | 65.1/19.3/0.3/15.3 ¹⁾ 65.5/19.6/0.4/14.6 ²⁾ 67.1/20.9/0.6/11.5 ³⁾ |
| Reactivity swing, pcm | 803 |
| Delayed neutron fraction (β_{eff}) | 0.00317 |
| Neutron generation time, μsec | 0.46 |
| Core power density, W/cc | 129 |
| Avg. linear power, W/cm | 193 |
| Fuel discharge burnup, a/o | 8.4 |
| Peak fast fluence, n/cm ² | 3.5x10 ²³ |
| Heavy metal consumption (U/TRU), kg/cycle | 196 / 92 |
| Heavy metal inventory (BOC/EOC), kg | 20,029 / 19,740 |
| BOC B-10 inventory, kg | 30.0 |
| LLFP loading (Tc-99/I-129), kg | 200 / 60 |
| LLFP transmutation (Tc-99/I-129), kg/cycle | 12.2 / 3.2 |
| LLFP discharge burnup (Tc-99/I-129), a/o | 48 / 42 |
| Void reactivity (100% active core), pcm | 3,462 |

¹⁾ Inner core, ²⁾ Middle core, ³⁾ Outer core

Basically, the TRU transmutation rate is not affected by the simultaneous incineration of LLFPs. Table VII shows that the average transmutation rates of Tc-99 and I-129 are fairly high, 6.9%/cycle and 6.0%/cycle, respectively, and their initial loadings are also relatively small. This good transmutation rate is largely attributed to the double-annular targets enclosing the moderator. As a result, the LLFP discharge burnup is relatively high for the 6-cycle irradiation. The LLFP discharge burnup could be further increased with a longer irradiation interval. It is observed that the fuel discharge burnup was reduced by about 7% since the fuel inventory was increased due to the LLFP

loading. However, the increased fuel inventory and transmutation of the LLFPs reduce the burnup reactivity swing a little. The reduced reactivity swing is attributed to factors, one is the higher fuel inventory and the other one is the depletion of LLFPs. It is worthwhile to note that transmutations of Tc-99 and I-129 lead to an increased reactivity because they are mainly transmuted to Ru-100 and Xe-130, which have significantly smaller absorption cross sections compared with their parent nuclides. Table VI also shows that the fuel enrichments are not very different in the three zones. It is expected that fabrication of these fuels would be feasible with the current fuel technologies. From Table VII, one can note that the LLFP transmutation in the reflector region substantially reduces the core void reactivity, about 20% reduction. More LLFP loading would lead to a further reduced core void reactivity.

In Fig. 5, the assembly power distribution is shown for the equilibrium cycle core. Peak assembly powers in the three zones are 5.17 MW, 5.45 MW, and 5.35 MW, respectively. Therefore, it is expected that the thermal-hydraulic analysis would give similar results as in Table IV for the TRU-only-loaded core since the assembly type is identical in each zone for the two cores.

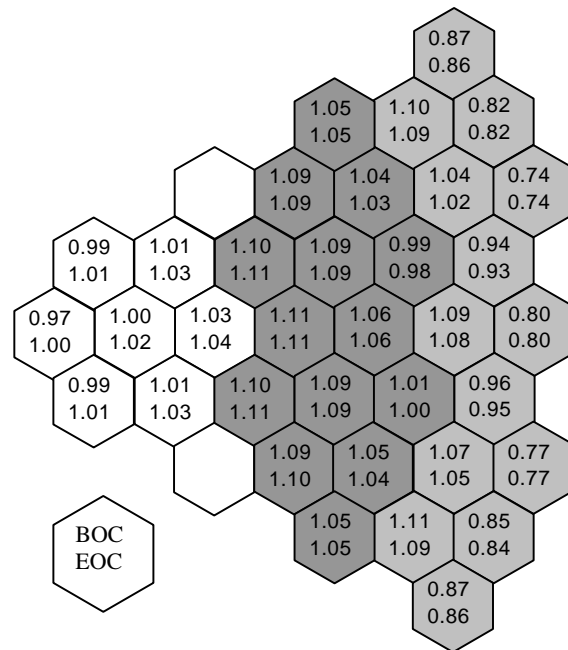


Fig. 5. Relative assembly power distribution in the core loaded with LLFP.

V. Conclusions and Future Works

Based on a proliferation-resistant practical closed fuel cycle, TRU and LLFP transmutation studies have been done in a 900 MWth lead-cooled fast reactor. It is assumed that only 97% uranium and 90% rare earth nuclides are removed from the nuclear spent fuel. It was found that the TRU transmutation capability of the core is about 1/3 (~92 kg/year) of an ideal TRU transmuter (~288 kg/year).

With the conventional core design concept based on fuel enrichment splitting, a lead-cooled TRU transmuter design is very challenging due to a large burnup reactivity swing and a high fast neutron fluence. As a solution to these problems, we introduced a new fuel assembly concept, where a B₄C burnable absorber rod with top/bottom cutbacks and a neutron streaming tube are placed. It was found that the burnup reactivity swing and the peak neutron fluence could be substantially reduced. With the aid of the new design features, it is possible to design a TRU-loaded core with a single fuel enrichment. However, introduction of the B₄C burnable absorber results in a significantly increased void reactivity.

A double-annular Tc-99/I-129 target enclosing a $ZrH_{1.78}$ moderator is an efficient design concept for the LLFP transmutation. It was found that a balanced simultaneous transmutation of both TRU and LLFP could be performed in the lead-cooled core without a serious trade-off in the core performance. Transmutation of both TRU and LLFP results in a ~7% reduced fuel discharge burnup. The transmutation rates of Tc-99 and I-129 are ~6.9%/year and ~6%/year, respectively. The study shows that a loading of LLFPs into the reflector zone substantially reduces the core void reactivity.

Acknowledgement

This work has been performed under the auspices of Korean Ministry of Science and Technology (MOST). The authors thank Dr. C. H. Cho for the thermal-hydraulic analysis with the MATRA code.

References

1. "Design of an Actinide Burning, Lead or Lead-Bismuth Cooled Reactor That Produces Low Cost Electricity," FY-02 Annual Report, MIT-ANP-PR-092 Rev 1, 2002.
2. W. S. Yang and H. S. Khalil, "Blanket Design Studies of a Lead-Bismuth Eutectic-Cooled Accelerator Transmutation of Waste System," *Nuclear Technology*, **135**, 162, 2001.
3. E. H. Kim, Private communication, Korea Atomic Energy Research Institute, 2003.
4. Y. Kim et al., "Self-Sustainable Lead-Cooled Reactor with Single Fuel Enrichment, to be published in ANS Transaction, 2003.
5. Y. Kim et al., "Core Design Characteristics of the HYPER System," OECD/NEA 7th Information Exchange Meeting on Actinide and Fission Product Partitioning & Transmutation, Jeju, Korea, 14-16 October, 2002.
6. B. J. Topel, "A User's Guide to the REBUS-3 Fuel Cycle Analysis Capability," ANL-83-2, Argonne National Laboratory, 1983.
7. K. L. Derstine, "DIF3D: A Code to Solve One-, Two-, and Three-Dimensional Finite Difference Diffusion Theory Problems," ANL-82-64, Argonne National Laboratory, 1984.
8. R. E. MacFarlane, "TRANSX2: A Code for Interfacing MATXS Cross Section Libraries to Nuclear Transport Codes," LA-12312-MS, Los Alamos National Laboratory, 1992.
9. R. E. Alcouffe et al., "User's Guide for TWODANT: A Code Package for Two-Dimensional, Diffusion-Accelerated Neutral Particle Transport," LA-10049-M, Los Alamos National Laboratory, 1990.
10. A. G. Croff, "A User's Manual for the ORIGEN2 Computer Code," ORNL/TM-7175, Oak Ridge National Laboratory, 1980.
11. Y. J. Yoo et al., "Development of a Subchannel Analysis Code MATRA Applicable to PWRs and ALWRs," *J. of the Korean Nuclear Society*, **31**, No. 3, 314, 1999.
12. Y. Kim et al., "Transmutation of Long-Lived Fission Products in Sodium-Cooled ATW System," OECD/NEA 7th Information Exchange Meeting on Actinide and Fission Product Partitioning & Transmutation, Jeju, Korea, 14-16 October, 2002.
13. H. J. Shim and C. H. Kim, "Monte Carlo Depletion Analysis of a PWR with the MCNAP," M&C 99 Int. Conf. On Mathematics and Computation, Reactor Physics and Environmental Analysis in Nuclear Application, Madrid, Spain, September, vol. 2, 1999.